

Influence of structural changes of $\text{Co}_{78}\text{Si}_9\text{B}_{13}$ metallic glass on magnetic properties

EWA JAKUBCZYK^{1*}, JÓZEF LELĄTKO², KATARZYNA PAWLIK³, ANNA PRZYBYŁ³

¹Institute of Physics, Jan Dlugosz University, al. Armii Krajowej 13/15, 42-200 Częstochowa, Poland

²Institute of Materials Science, University of Silesia, Bankowa 12, 40-007 Katowice, Poland

³Institute of Physics, Częstochowa University of Technology, al. Armii Krajowej 19, 42-200 Częstochowa, Poland

*Corresponding author: e.jakubczyk@ajd.czest.pl

The primary crystallization of $\text{Co}_{78}\text{Si}_9\text{B}_{13}$ metallic glass starts at 648 K and as a consequence of this the ϵ -Co(Si) phase with needle morphology is created. The second stage of crystallization (at 773 K) is the eutectic and as a result of this α -Co(Si) and boron phases: $(\text{Co},\text{Si})_3\text{B}$, $(\text{Co},\text{Si})_2\text{B}$ are formed. The crystallites of these phases have layer morphology. These characteristic morphologies in the first and second stages lead to the increase in coercivity.

Keywords: metallic glass, crystallization, coercivity.

1. Introduction

When the first metallic glasses were obtained, their stability became a problem [1–3]. Metallic glasses are in the metastable state and under the influence of different stimulating factors (*e.g.*, annealing at different temperatures or isothermal annealing during different time intervals and annealing by contribution of additional conditions as magnetic field, stress) they evolve with different rate to the stable polycrystalline state. Depending on their composition, the process of crystallization proceeds through one or many stages and through various crystallizations: primary, eutectic, polymorphous or perytectic [4]. As a result of crystallization, the properties of the metallic glasses change, which is undesirable from the application point of view of these materials in the amorphous state. Therefore, it is necessary to investigate the process of crystallization in connection with their properties changes. The knowledge of crystallization will define the safe range of temperature for correct work of devices. The control of the kinetics of the crystallization and microstructure could let obtain the metallic alloys with defined properties. The complete or partial crystallization of the amorphous alloys lets obtain materials with structure and properties which cannot be obtained in a different way, *e.g.*, nanocrystalline alloys of types: FINEMET, NANOPERM, HITPERM [5–8].

The investigation of the $\text{Co}_{78}\text{Si}_9\text{B}_{13}$ metallic glass presented in this paper is a continuation of the investigations from papers [9, 10]. Progressive process of crystallization was thermally stimulated and this way stated the sequence of the creation of the crystalline phases from the amorphous matrix by means of X-ray diffraction and transmission electron microscopy (TEM). The results of the influence of the structural changes on the properties were presented for important applicational parameters, *i.e.*, saturation magnetization, remanence and coercivity.

2. Experiment

The $\text{Co}_{78}\text{Si}_9\text{B}_{13}$ metallic glass was prepared by the roller quenching method in the Institute of Materials Engineering of Warsaw Technical University, Poland.

Measurements of X-ray diffraction were done at the room temperature for the as-received as well as isochronally (4 h) annealed samples at various temperatures (573–823 K) and for the isothermally (648 K) annealed samples during different time intervals (10^4 – 2×10^4 s). The X-ray studies were performed using a DRON-2.0 diffractometer with a horizontal goniometer of GUR-5 type. The X-ray tube had a molybdenum target ($\lambda_{\text{K}\alpha} = 0.71069 \times 10^{-10}$ m) and a graphite monochromator in the primary beam.

The microstructure and phase composition were studied by TEM using JEOL-JEM 3010 microscope with EDS detector. Thin foils for TEM were prepared by ion polishing.

The magnetic properties were determined from the measured hysteresis loops at room temperature using a vibration sample magnetometer (VSM-Lake Shore) operating in a magnetic field up to 2 T. From the hysteresis loops for samples non-annealed as well as annealed at 648 K and 823 K the values of magnetic parameters like coercivity, remanence and saturation magnetization were determined.

3. Results and discussion

The X-ray and TEM investigations of $\text{Co}_{78}\text{Si}_9\text{B}_{13}$ metallic glass were performed to analyse the structural changes and identify the crystalline phases formed in the transformation from the parent amorphous matrix to the polycrystalline one. The X-ray diffractions were made for the non-annealed as well as annealed samples (Fig. 1a). The X-ray diffraction performed for the samples annealed at different temperatures (573–823 K) during 4 h allowed to observe the occurring structural changes. It was stated that after the annealing at the temperature of 648 K the metallic glass starts the primary crystallization, and the crystallizing phase is the hexagonal ϵ -Co(Si) [11]. This was proved by the X-ray diffraction patterns (Fig. 1b) obtained for the samples annealed isothermally at this temperature in different times (from 10^4 to 2×10^4 s).

The quality phase analysis proved the existence of the crystalline metallic phase of type α -Co(Si) as well as the boron phases: $(\text{Co},\text{Si})_2\text{B}$, $(\text{Co},\text{Si})_3\text{B}$ and a small part of the metallic phase of type ϵ -Co(Si) after the final annealing (823 K) [11, 12].

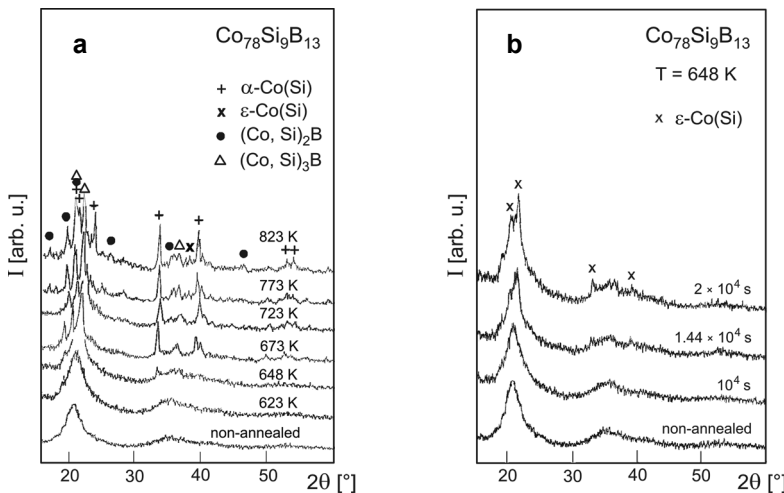


Fig. 1. X-ray diffraction pattern for samples of the $\text{Co}_{78}\text{Si}_9\text{B}_{13}$ alloy annealed: at different temperatures **(a)**, during different time intervals at 648 K **(b)**.

The creation of the metallic phase α -Co(Si) and boron phases is a result of the eutectic crystallization, which occurs after the annealing at the temperature of 773 K. The trace amount of the phase ε -Co(Si) can be explained by the polymorphous reaction, which results in transformation of the phase ε -Co(Si) into α -Co(Si) phase. This transformation correlates with the phase diagram Co-Si, which shows that 420 °C is the temperature of transformation: ε -Co(Si) \rightarrow α -Co(Si) [13].

The pictures of the microstructure obtained by the electron microscopy for the samples after the annealing at the 648 K and 823 K show different morphology of the crystallites. These are crystallites with needle morphology (Fig. 2) and a numerous

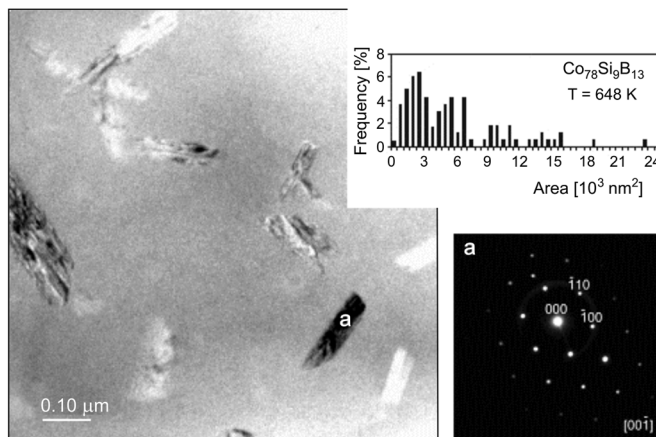


Fig. 2. TEM micrograph for the sample of the $\text{Co}_{78}\text{Si}_9\text{B}_{13}$ alloy annealed at 648 K for 4 h and grain size distribution, **a** – the electron diffraction pattern for ε -Co(Si) [11].

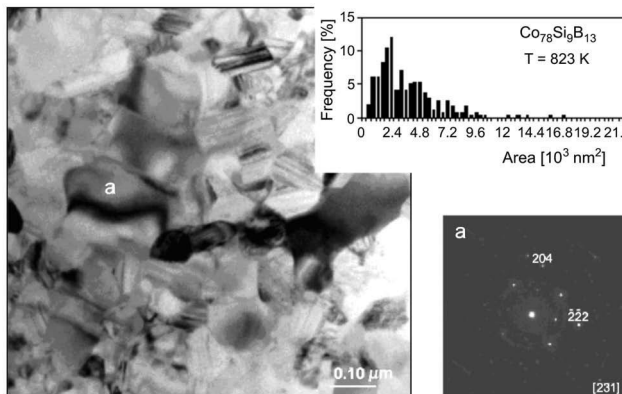


Fig. 3. TEM micrograph for the sample of the Co₇₈Si₉B₁₃ alloy annealed at 823 K for 4 h and grain size distribution, *a* – the electron diffraction pattern for Co₂Si [14].

group with layer morphology (Fig. 3). The latter ones are polycrystallites of fused crystallites from the early stage of crystallization and the ones growing in the second stage of crystallization.

The values of the magnetic parameters (coercivity, remanence and saturation magnetization) obtained from the hysteresis loops for samples non-annealed as well as annealed at 648 K and 823 K are listed in the Table.

The increase in coercivity after annealing at 648 K and 823 K corresponds to Herzer diagram for the nanocrystallites, according to which: $H_c \propto D^6$ (D – average diameter grain) [15]. The obtained values of coercivity and the average grain

Table. The magnetic parameters for the Co₇₈Si₉B₁₃ alloy.

Annealed	JH_c [kA/m]	M_s [Am ² /kg]	M_r [Am ² /kg]
Non-annealed	0.15	104.14	0.48
648 K	7.34	82.88	6.69
823 K	40.43	90.23	19.92

diameters show the following dependences: $(JH_c, 823\text{ K})/(JH_c, 648\text{ K})^{1/6} = 1.33$ and $\overline{D}_{823\text{ K}}/\overline{D}_{648\text{ K}} \approx 1.31$. They agree with Herzer diagram. A big increase in coercivity is caused by the characteristic morphology of the created crystallites during crystallization, the needle one after the first stage (Fig. 2) and the layer one after the second stage (Fig. 3).

4. Conclusions

Based on the results presented we can formulate the following conclusions:

- The crystallization of Co₇₈Si₉B₁₃ metallic glass proceeds through two main stages with different types of reactions: primary (648 K) and eutectic (773 K).

- The hexagonal metallic phase ϵ -Co(Si) created after the first stage of crystallization transforms through the polymorphous reaction into regular phase α -Co(Si).
- Both stages of the crystallization are accompanied by different morphologies of the crystallites: needle and layer in the first and the second stages of crystallization, respectively.
- The characteristic morphology of the crystallites is responsible for the increase in coercivity.

References

- [1] KLEMENT W. JR., WILLENS R.H., DUWEZ P., *Non-crystalline structure in solidified gold–silicon alloys*, Nature **187**, 1960, pp. 869–870.
- [2] DUWEZ P., WILLENS R.H., CREWDSON R.C., *Amorphous phase in palladium–silicon alloys*, Journal of Applied Physics **36**(7), 1965, pp. 2267–2269.
- [3] DUWEZ P., LIN S. C.H., *Amorphous ferromagnetic phase in iron–carbon–phosphorus alloys*, Journal of Applied Physics **38**(10), 1967, pp. 4096–4097.
- [4] KÖSTER U., *Phase transformations in rapidly solidified alloys*, Key Engineering Materials **81–83**, 1993, pp. 647–662.
- [5] YOSHIZAWA Y., OGUMA S., YAMAUCHI K., *New Fe-based soft magnetic alloys composed of ultrafine grain structure*, Journal of Applied Physics **64**(10), 1988, pp. 6044–6046.
- [6] MAKINO A., BITOCH T., INOUE A., MASUMOTO T., *Nanocrystalline Fe–M–B–Cu ($M = Zr, Nb$) alloys with improved soft magnetic properties*, Journal of Applied Physics **81**(6), 1997, pp. 2736–2739.
- [7] WILLARD M.A., LAUGHLIN D.E., McHENRY M.E., THOMA D., SICKAFUS K., CROSS J.O., HARRIS V.G., *Structure and magnetic properties of $(Fe_{0.5}Co_{0.5})_{88}Zr_7B_4Cu_1$ nanocrystalline alloys*, Journal of Applied Physics **84**(12), 1998, pp. 6773–6777.
- [8] McHENRY M.E., WILLARD M.A., LAUGHLIN D.E., *Amorphous and nanocrystalline materials for applications as soft magnets*, Progress in Materials Science **44**(4), 1999, pp. 291–433.
- [9] JAKUBCZYK E., STĘPIEŃ Z., JAKUBCZYK M., *Influence of the composition of $M_{78}Si_9B_{13}$ metallic glasses on their structural stability*, Optica Applicata **35**(3), 2005, pp. 339–346.
- [10] JAKUBCZYK E., *Phase transitions in $Co_{78}Si_9B_{13}$ and $Fe_{78}Si_9B_{13}$ metallic glasses induced by isochronal annealing*, Materials Science – Poland **24**(4), 2006, pp. 1027–1036.
- [11] TAYLOR A., FLOYD R.W., *Precision measurements of lattice parameters of non-cubic crystals*, Acta Crystallographica **3**(4), 1950, pp. 285–289.
- [12] HAVINGA E.E., DAMSMA H., HOKKELING P., *Compounds and pseudo-binary alloys with the $CuAl_2(C16)$ -type structure. I. Preparation and X-ray results*, Journal of the Less-Common Metals **27**(2), 1972, pp. 169–186.
- [13] MASSALSKI T., *Binary Alloy Phase Diagrams*, American Society for Metals, Metals Park, Ohio 1986, p. 801.
- [14] YANMING ZHAO, JINGKUI LIANG, GUANGHUI RAO, YONGQUAN GUO, WEIHUA TANG, CHENG DONG, FEI WU, *Phase relations in the Nd–Co–Si system at 800 °C*, Journal of Alloys and Compounds **241**(1–2), 1996, pp. 191–195.
- [15] HERZER G., *Grain size dependence of coercivity and permeability in nanocrystalline ferromagnets*, IEEE Transactions on Magnetics **26**(5), 1990, pp. 1397–1402.

Received June 23, 2009